Charge Scan Reveals an Extended Region at the Intracellular End of the GABA Receptor Pore that Can Influence Ion Selectivity

Virginia E. Wotring[1] and David S. Weiss[2]

[1]Department of Neurobiology, University of Alabama at Birmingham, Birmingham, AL 35294
[2]Department of Physiology, University of Texas Health Science Center at San Antonio, San Antonio, TX 78229

Selective permeability is a fundamental property of ion channels. The Cys-loop receptor superfamily is composed of both excitatory (ACh, 5-HT) and inhibitory (GABA, glycine) neurotransmitter-operated ion channels. In the GABA receptor, it has been previously shown that the charge selectivity of the integral pore can be altered by a single mutation near the intracellular end of the second transmembrane-spanning domain (TM2). We have extended these findings and now show that charge selectivity of the anionic ρ1 GABA receptor can be influenced by the introduction of glutamates, one at a time, over an 8–amino acid stretch (−2′ to 5′) in the proposed intracellular end of TM2 and the TM1–TM2 intracellular linker. Depending on the position, glutamate substitutions in this region produced sodium to chloride permeability ratios ($P_{Na}+/_{Cl}-$) varying from 0.64 to 3.4 (wild type $P_{Na}+/_{Cl}- = 0$). In addition to providing insight into the mechanism of ion selectivity, this functional evidence supports a model proposed for the homologous nicotinic acetylcholine receptor in which regions of the protein, in addition to TM2, form the ion pathway.

INTRODUCTION

Discrimination among ions is a critical function of ligand-gated ion channels. The Cys-loop receptor superfamily, which includes nicotinic acetylcholine (nACh), γ-aminobutyric acid ($GABA_A$ and $GABA_C$), glycine, and serotonin ($5\text{-}HT_3$) receptors, has lent itself to the study of selectivity because its members have similar amino acid sequences, but opposing charge selectivities. Examination of Cys-loop receptor sequences, and comparisons of permeabilities among wild-type and mutant Cys-loop receptors, has suggested that selectivity is regulated by charged amino acid residues in a few key positions where they interact with ions as they traverse the channel pore (Konno et al., 1991; Galzi et al., 1992; Keramidas et al., 2000; Gunthorpe and Lummis, 2001; Jensen et al., 2002).

After the original determination of the second transmembrane domain (TM2) being the major pore-forming region (Giraudat et al., 1986; Hucho et al., 1986; Leonard et al., 1988), studies have focused on the −2, −1′, and 13′ residues as determinants of ionic selectivity (Cohen et al., 1992a,b; Galzi et al., 1992; Keramidas et al., 2000; Gunthorpe and Lummis, 2001; Jensen et al., 2002; Thompson and Lummis, 2003). In this numbering scheme, 0′ would be the presumed intracellular end of TM2 (Fig. 1 A), although there is no strong evidence placing this arginine in the membrane or in the cytoplasm. Changing the −2′, −1′, and 13′ residues in a cationic channel to the corresponding amino acids found in an anionic channel (Fig. 1 B) can reverse selectivity (Galzi et al., 1992). In a previous study of the ρ1 subunit, we examined the reverse mutations including alanine to glutamate at the −1′ position. This mutant channel did not distinguish between anions and cations, although we found that glutamate substitution of the 0′ residue resulted in a reversal of selectivity (Wotring et al., 2003). In MOD-1, a serotonin-gated chloride channel cloned from *Caenorhabditis elegans*, this same substitution caused a charge reversal in ion selectivity (Menard et al., 2005).

To expand on this result and to understand the impact of negative charges in the pore region, we made mutants to systematically slide this presumed glutamate ring either toward the extracellular end of TM2 or in the opposite direction toward TM1. The permeability changes imparted by these mutations allowed us to locate critical elements of the selectivity filter at the intracellular mouth of the channel pore.

MATERIALS AND METHODS

cDNA Cloning and In Vitro Transcription

The cDNA encoding the human ρ1 wild-type subunit (accession no. NM 002042) was cloned into pGEMHE (Liman et al., 1991) for expression in *Xenopus laevis* oocytes. Point mutants were produced in ρ1 using the PCR overlap extension method (Kammann et al., 1989). Glutamate was substituted for the native amino acid at positions −12′ to 20′ of the TM2 numbering system (amino acid residues 280–312 in ρ), for a total of 33 glutamate mutants, 26 of which formed functional GABA-activated receptors.

Correspondence to David S. Weiss: weissd@uthscsa.edu

Abbreviations used in this paper: nACh, nicotinic acetylcholine; SCAM, substituted cysteine accessibility method; TM2, second transmembrane domain.

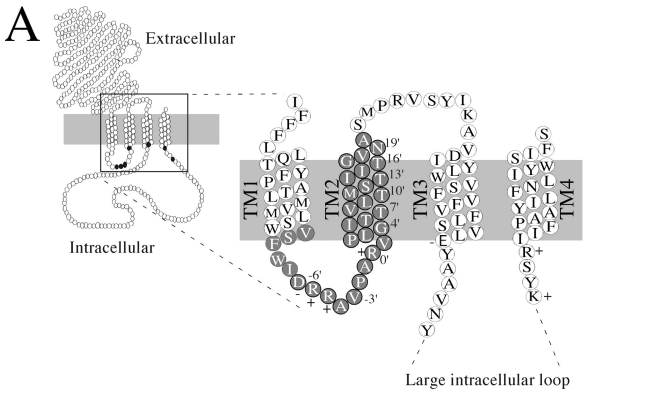

Figure 1. Diagram of proposed ρ1 GABA receptor subunit topology and transmembrane domain sequences. (A) Endogenously charged residues are indicated by the appropriate charge sign and these residues were neutralized in this study to examine the role of endogenous charges on ionic selectivity. The TM2 numbering system used in the manuscript begins with the 0' TM2 arginine with increasing numbers proceeding toward the C terminus. Charge-scanning mutants covered the region from −12' (intracellular valine, V) to 20' (extracellular alanine, A) and are indicated with gray-filled circles. This figure is to merely show the extent of the residues examined in this study and the secondary structure or positions of these residues with respect to the membrane should not be taken literally. (B) Aligned TM1–TM2 linker and TM2 sequences from several representative members of the receptor family. Anionic members are above the dashed line, cationic members are below. The GABA ρ1 receptor sequence is human, all others are rat.

In one case of a nonfunctional glutamate substitution (A288E), we substituted aspartate (also negatively charged) instead of glutamate. A neutral amino acid (alanine, glycine, or methionine) was systematically substituted for most of these positions in an attempt to control for effects of mutagenesis at these sites. Additionally, the positively charged lysine was substituted for −5′ to 2′, to examine the effects of side chain charge at these particular positions. The cDNA for each construct was linearized, and cRNA was synthesized using standard in vitro transcription techniques as described previously (Amin and Weiss, 1994). Yield and integrity of cRNA were verified by agarose gel electrophoresis. Unless specified, all chemicals were purchased from Sigma-Aldrich.

Oocyte Preparation and Microinjection

Female *Xenopus laevis* (*Xenopus* I) were anesthetized with 0.2% MS-222, and several lobes of ovary were surgically removed in a procedure approved by the UAB Institutional Animal Use and Care Committee. The incision was sutured, and the animal was monitored during its recovery period for 1 wk, after which it was returned to its tank. Ovarian lobes were placed in a calcium-free oocyte Ringer (OR2) that consisted of (in mM) NaCl, 92.5; KCl, 2.5; $MgCl_2$, 1; Na_2HPO4, 1; HEPES, 5; penicillin, 50 U/ml; streptomycin, 50 μg/ml; pH 7.5. The ovarian lobes were cut into small pieces, and then digested in 0.3% collagenase A (Boehringer Mannheim) in the above solution. After dispersal for ∼2 h, stage VI oocytes were selected and thoroughly rinsed and maintained in OR2 with $CaCl_2$ (1 mM) at 18°C for several hours before cRNA injection. Typically, 60–100 nl of cRNA (25–100 ng/μl) was injected into the oocyte with a Nanoject (Drummond Scientific), and then the oocytes were incubated at 16°C for 1–5 d. Oocytes were screened in voltage-clamp for expression of GABA receptors. Low expression levels (GABA-induced currents between 200 and 1,000 nA) were used for reversal potential experiments in order to minimize the error due to series resistance (<4% with 1,000 nA current).

Voltage-Clamp Experiments

The oocyte was placed in a small volume chamber with a continuous perfusion system, as described previously (Amin and Weiss, 1994). The normal extracellular OR2 consisted of (in mM) NaCl, 92.5; KCl, 2.5; $MgCl_2$, 1; $CaCl_2$, 1; HEPES, 5; pH 7.5. Recording microelectrodes were fabricated from thin-walled glass micropipettes (A-M Systems) on a Sutter P87 horizontal puller and filled with 3 M KCl (resistance = 1–3 MΩ). The ground electrode was placed in a separate 3 M KCl well connected to the bath by an agar bridge, in order to prevent errors due to junction potentials during ion substitution experiments. Solutions for ion replacement experiments had a portion of the usual NaCl replaced with an isoosmotic amount of sodium isethionate or TEA chloride. For the determination of agonist sensitivity, dose–response relationships were fitted with the following form of the Hill equation:

$$\text{Activation} \quad I = \frac{I_{max}}{1 + \left(EC_{50}/[A]\right)^{n_H}}, \qquad (1)$$

where I_{max} is the maximum GABA-activated current, EC_{50} is the concentration of GABA required to reach half the maximum, and n_H is the Hill coefficient.

Reversal Potential Measurements

Each oocyte was allowed to equilibrate at a holding potential of −70 mV in each solution for approximately 1 min before recording sequences were begun. A group of five voltage ramps was applied from −70 to +10 mV and then averaged. Each individual ramp lasted 1 s with 3-s intervals between ramps. The solution was then switched to a GABA-containing solution with the same ionic composition. When the GABA response reached steady state, five more ramps were taken and averaged. This was followed by a third set of ramps after complete recovery from the GABA application. Reversal potential was determined by averaging the initial and recovery ramps, and this average control ramp was subtracted from the average ramp during GABA application. The voltage at which this ramp crossed the abscissa was the reversal potential of the GABA-induced portion of the current. Reversal potentials were measured in OR2 at the beginning and end of each experiment and were typically identical, indicating that the internal ion concentrations remained stable, even though the extracellular ion concentrations were changed many times during the course of the experiment. In the few cases where a difference was observed, those particular experiments were discarded. In all cases, GABA (Calbiochem) was applied at the concentration required for half-maximal activation (EC_{50}).

Data Analysis

The permeabilities (P) of other ions relative to chloride were calculated using the Goldman Hodgkin-Katz equation (Goldman, 1943; Hodgkin and Katz, 1949) with internal ion activities used

previously (Wotring et al., 2003) and the known activities for external chloride and replacement ions. Least squares fitting was used (Igor, Wavemetrics) to calculate the ionic permeability coefficients from the following equation, using reversal potentials measured at various activities of extracellular chloride and sodium:

$$f(x,y) = -58\log\frac{P_{Na}[Na^+]_i + P_K[K^+]_i + P_{Cl}[x]_o}{P_{Na}[y]_o + P_K[K^+]_o + P_{Cl}[Cl^-]_i}. \quad (2)$$

Permeability coefficients for sodium and potassium were fit simultaneously (holding P_{Cl-} at one for normalization) with reversal potentials measured in OR2 and three different sodium concentrations and three different chloride concentrations. Data from five to seven individual cells were fit separately. The resulting permeability values were then averaged and the standard error was calculated. A Student's *t* test was applied to determine significant differences from wild type, using $P < 0.05$.

Estimating Pore Size

We made substitutions with a range of anions and cations of different dimensions to determine the cutoff and estimate pore size. For these experiments, 50 mM of the NaCl was replaced with 50 mM of the test solution and reversal potentials were obtained as described previously. Using the permeability coefficients determined for each mutant receptor and Eq. 2, we calculated the theoretical reversal potential shift expected for the 50 mM substitution of the impermeant ion. In theory, substitution by an impermeant ion will reduce the concentration of the permeant ion and shift the measured reversal potential to this predicted value. If the reversal potential shift is significantly less than this theoretical value, the substituted ion is permeant. The cations and their diameters (in Å) used in this study were sodium, 1.9; rubidium, 3.0; cesium, 3.4; imadazole, 4.8; choline, 5.6; triethanolamine, 7.0; *N*-methyl-D-glucamine, 9.0; and the anions and their diameters were bromide, 2.4; chloride, 2.4; formate, 3.4; bicarbonate, 4.1; acetate, 4.5; propionate, 5.1; gluconate, 6.9; isethionate, 7.0 (Marcus, 1997).

RESULTS

Recently, we have shown that glutamate substitution of the conserved positively charged residue at 0' (ρ1 R292, Fig. 1 A) can reverse the ionic selectivity of GABA receptors (Wotring et al., 2003), expanding upon previous studies showing the neighboring −1' residue is critical for ionic charge selectivity (Galzi et al., 1992; Keramidas et al., 2000; Gunthorpe and Lummis, 2001; Jensen et al., 2002; Thompson and Lummis, 2003; Menard et al., 2005). This result suggested that other residues, in addition to −1', can affect ion selectivity. We set out to determine the spatial extent of the domain that can alter selectivity with a charge-scanning mutagenesis method, i.e., by making charge-substitution mutants to systematically scan the pore region.

Residues in and near the pore region of the ρ1 GABA subunit were mutated to negative (glutamate: E, or aspartate: D), positive (lysine: K), or neutral amino acids (alanine: A, or glycine: G). Since the ρ1 GABA subunit forms functional homomeric receptors, each mutant homopentamer actually contained five mutant residues. Of the 51 mutant GABA receptors constructed for this study, all but 10 responded to GABA application and three mutants produced high baseline currents (>1 μA) independent of agonist application that precluded them from further experimentation. Fig. 2 shows GABA-activated currents in the wild-type receptor and four individual glutamate mutants. The dose–response relationships are plotted in Fig. 2 B. These particular mutations are in the region that we will show has the largest impact on selectivity. Note that three of the mutations (P290E, V293E, and P294E) imparted a four- to fivefold decrease in agonist sensitivity evident as a rightward shift in the dose–response relationship. R292E was similar in sensitivity to the wild-type receptor. Table I provides the parameters determined from fitting the Hill equation (see Materials and methods) to the dose–response relations for all the mutants in this study. The majority of the mutants showed functional characteristics (dose–response relationship, activation and deactivation kinetics) similar to the wild-type receptor, suggesting we have likely not perturbed structures crucial to receptor activation.

Is the Selectivity Filter Limited to the −1′ Residue?

As seen in Fig. 3 A, the P290E mutant conducted cations better than anions. The reversal potential in a low Cl^- solution (solid trace) is about the same as in normal OR2 (indicated by the arrow), but there is a large negative shift in low Na^+ (dashed trace). Reversal potentials were determined in several sodium and chloride concentrations. The rightmost graphs in Fig. 3 plot these reversal potentials as a function of sodium (filled circles) and chloride (open circles) concentrations. For P290E the fitted permeability coefficients were $P_{Na+/Cl-} = 3.4 \pm 1.2$ and $P_{K+/Cl-} = 2.1 \pm 0.7$. These results are in stark contrast to those obtained with our two other mutations at the same site (Fig. 3, B and C). Substitution of neutral alanine for proline had a limited effect on permeability ($P_{Na+/Cl-} = 0.05 \pm 0.06$ and $P_{K+/Cl-} = 0.06 \pm 0.03$, $n = 5$). For comparison, the wild-type ρ1 receptor exhibits a $P_{K+/Cl-}$ of 0.03 ± 0.02 and a $P_{Na+/Cl-}$ of 0 (Wotring et al., 2003). Substitution of a positively charged lysine residue had a modest, but significant, effect on permeability ($P_{Na+/Cl-} = 0.09 \pm 0.04$ and $P_{K+/Cl-} = 0.13 \pm 0.02$, $n = 5$), although changes in rectification were apparent. These data from the −2' site, together with our previous results from the −1' and 0' mutants (Wotring et al., 2003), suggested there are a number of locations in this region that can influence selectivity. The data in Fig. 3 also demonstrate that the addition of negative charges to an anionic channel at this site can impart permeability to cations, while the presence of positive charges or neutral amino acids has a minimal impact on selectivity. The observation that neutral or positive substitutions do alter the selectivity profile to some extent indicates that there are changes in structure that go beyond the electrostatic modifications.

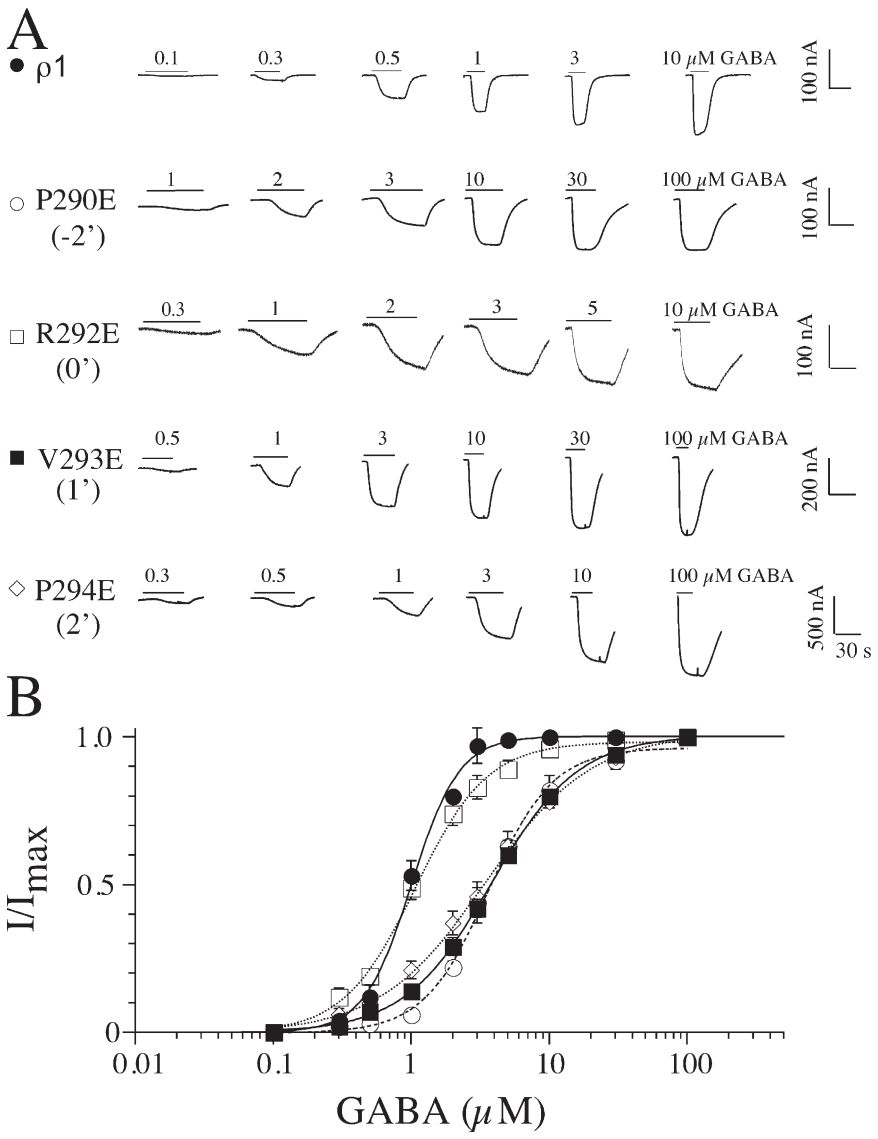

Figure 2. Dose–response relationships for selected glutamate scan mutants. (A) GABA-gated currents at a range of agonist concentrations in oocytes expressing the indicated mutants are shown. (B) Maximum current amplitudes were plotted as a function of GABA concentration and fitted with the Hill equation (Eq. 1 in Materials and methods). Parameters from these fits are provided in Table I. In general, the mutations had a modest effect on agonist sensitivity.

What Is the Spatial Range of the Region Where Ion Charge Selectivity Can Be Reversed?

Continuation of the glutamate scan shows that while the −2' and 0' sites are the most cation selective when mutated to glutamate, five additional glutamate substitutions (−1', 1', 2', 3′, and 5′) produced receptors that were essentially nonselective (Fig. 4). The permeability profiles in Fig. 4 show an alternating pattern from −2' to 2'. This pattern is more evident in Fig. 5 where the sodium (Fig. 5 A) and potassium (Fig. 5 B) permeabilities (shown as a ratio to chloride) are plotted for the glutamate scan. This result prompted us to extend the glutamate scan away from this region in both directions, but it was evident that only glutamate mutations from −2' to 5′ resulted in cation or nonselective pores (Fig. 5).

Since substitution of negatively charged residues resulted in increased permeability to cations, we substituted positively charged lysine to examine the effect of the reverse charge at the same sites. Most of the lysine mutants showed little to no difference in permeability from wild type. (Fig. 5, gray symbols). Neutralization of the same residues by alanine substitution also had a limited effect on ionic permeabilities (Fig. 5, open symbols). The reversal of ionic selectivity was unique to glutamate substitutions.

Do Endogenous Charged Residues Play a Role in Selectivity?

Examination of the wild type ρ1 sequence shows a number of charged residues near the intracellular membrane interface (Fig. 1), possibly in a position to interact with permeating ions. We systematically neutralized these charged residues to test their role in selectivity. Neutralization of individual sites had little to no effect on ionic permeabilities ($P_{K+/Cl-} < 0.10$; Fig. 6). No additional cationic permeability was seen when multiple substitutions were made in the same subunit. These results demonstrate that these endogenous charged residues

TABLE I

Wild-Type and Mutant GABA Concentration–Response Relationships

E Mutants				K Mutants				Neutral Mutants			
Mutant	EC_{50}	Hill slope	*n*	Mutant	EC_{50}	Hill slope	*n*	Mutant	EC_{50}	Hill slope	*n*
ρ1	0.8 ± 0	3.4 ± 0.1	8								
V280E (−12')	4.7 ± 0.5	1.1 ± 0.1	5								
S281E (−11')	1.0 ± 0.1	1.6 ± 0.1	5								
F282E (−10')	NFE		30								
W283E (−9')	NFE		30								
I284E (−8')	2.8 ± 0.2	2.0 ± 0.1	5								
D285E (−7')	1.0 ± 0.1	2.3 ± 0.3	5					D285N	1.8 ± 0.4	1.8 ± 0.2	6
R286E (−6')	0.3 ± 0.0	2.5 ± 0.3	5					R286M	0.6 ± 0.1	2.9 ± 0.1	6
R287E (−5′)	1.0 ± 0.1	3.0 ± 0.3	4	R287K	24.0 ± 2.6	2.4 ± 0.8	5	R286Q/R287Q	0.4 ± 0.03	2.8 ± 0.5	6
A288D (−4')	1.5 ± 0.2	2.4 ± 0.2	5	A288K	2.3 ± 0.4	2.3 ± 0.3	5	A288G	2.6 ± 0.3	1.4 ± 0.1	5
V289E (−3′)	1.3 ± 0.1	2.1 ± 0.1	5	V289K	4.4 ± 0.5	1.1 ± 0.1	5	V289A	4.8 ± 0.3	2.1 ± 0.1	5
P290E (−2')	4.1 ± 0.3	1.8 ± 0.2	6	P290K	19.4 ± 1.9	1.4 ± 0.3	5	P290A	2.8 ± 0.1	1.1 ± 0.1	6
A291E (−1')	2.0 ± 0.1	1.9 ± 0.1	5	A291K	2.0 ± 0.1	1.9 ± 0.1	5	A291G	1.6 ± 0.2	2.7 ± 0.2	5
R292E (0')	1.3 ± 0.1	1.4 ± 0.2	5	R292K	11.9 ± 1.3	0.7 ± 0.1	5	R292M	1.8 ± 0.1	1.0 ± 0.1	6
V293E (1')	3.9 ± 0.3	1.4 ± 0.1	5	V293K	0.6 ± 0.1	1.3 ± 0.1	5	V293A	2.3 ± 0.2	2.1 ± 0.2	5
P294E (2')	3.3 ± 0.2	1.2 ± 0.1	5	P294K	0.07 ± 0.01	1.0 ± 0.1	5	P294A	2.4 ± 0.6	2.0 ± 0.3	5
L295E (3′)	1.6 ± 0.2	1.9 ± 0.4	5					L295A	1.6 ± 0.2	1.6 ± 0.2	5
G296E (4')	1.4 ± 0.1	2.1 ± 0.2	5	G296K	NFE		30	G296A	2.4 ± 0.1	1.6 ± 0.2	5
I297E (5′)	4.7 ± 0.2	1.0 ± 0.1	5	I297K	NFE		30	I297A	1.5 ± 0.1	2.1 ± 0.1	5
T298E (6')	NFE		30	T298K	NFE		30	T298A	1.4 ± 0.2	1.9 ± 0.2	5
T299E (7')	1.2 ± 0.1	1.8 ± 0.2	5	T299K	NFE		30	T299A	2.2 ± 0.2	1.7 ± 0.1	5
V300E (8')	NFE		30								
L301E (9')	2.1 ± 0.4	1.5 ± 0.4	5	L301K	HL		30				
T302E (10')	HL		30	T302K	HL		30				
M303E (11')	0.7 ± 0.1	2.4 ± 0.2	5								
S304E (12')	1.2 ± 0.1	2.3 ± 0.2	5					S304A	0.9 ± 0.1	2.7 ± 0.3	5
T305E (13')	0.06 ± 0.008	2.7 ± 0.3	5					T305A	0.2 ± 0.05	2.7 ± 0.3	5
I306E (14')	NFE							I306A	0.3 ± 0.1	2.3 ± 0.2	5
I307E (15')	NFE							I307A	0.1 ± 0.01	1.4 ± 0.2	5
T308E (16')	0.7 ± 0.1	3.1 ± 0.1	5								
G309E (17')	0.02 ± 0.003	1.46 ± 0.1	5								
V310E (18')	0.06 ± 0.01	1.84 ± 0.1	5					V310A	1.9 ± 0.1	2.3 ± 0.1	5
N311E (19')	0.6 ± 0.05	2.3 ± 0.3	5					N311A	0.7 ± 0.1	2.8 ± 0.3	5
A312E (20')	0.2 ± 0.01	3.1 ± 0.3	5					D285N/R286Q/R287Q/R292M	1.6 ± 0.2	2.0 ± 0.2	6

Values are mean ± SEM with *n* equal to the number of oocytes tested. Note that most charge neutralization or glutamate substitutions had little effect on the agonist dose–response curve, while some lysine mutations resulted in modest increases in the GABA EC_{50}. Constructs that failed to exhibit currents upon application of GABA are indicated by NFE (no functional expression). Constructs that exhibited small (<100 nA) currents with a concomitant high background (>1 μA) are labeled HL (high leak). The glutamate substitution mutant A288E was nonfunctional; results from an aspartate substitution mutant (A288D) are reported for this position.

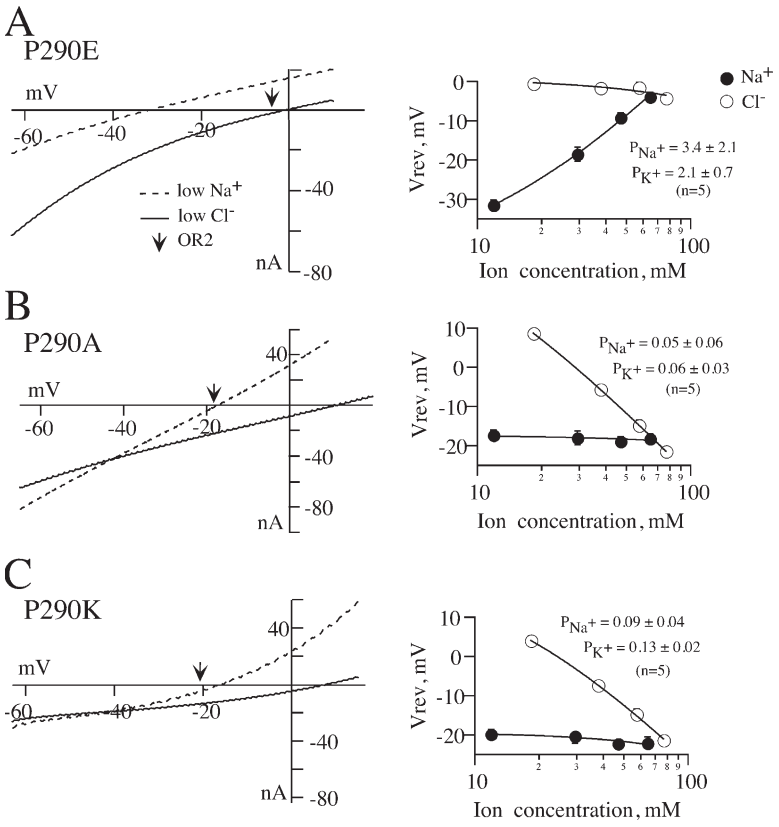

Figure 3. A negatively charged substitution at P290 (−2') results in cation-preferring receptors. (A) Amplitudes of GABA-induced currents from P290E were measured at a continuously varying membrane potential using the ramp protocol described in the Materials and methods. Ramps obtained in low sodium OR2 are the dashed lines and those in low-chloride OR2 are the solid lines. The normal OR2 ramp is omitted for clarity, but the reversal potential is indicated with an arrow. For the graph on the right, reversal potentials were measured at different concentrations of sodium (solid) or chloride (open) and fit with the GHK equation (Eq. 2) to determine the relative permeability coefficients. Substitution of negatively charged glutamate for the native proline at position 290 (−2') resulted in cation-preferring receptors, but receptors were chloride selective when this site was mutated to neutral alanine (B) or positively charged lysine (C).

were not among the primary determinants of ion selectivity in the wild-type ρ1 receptor.

Do the Mutations Alter the Pore Diameter?

The finding that, via site-directed mutagenesis, we could create a receptor that was equally permeant to both anions and cations, suggested that we may have produced a permeation pathway of larger than normal physical dimensions. To test this possibility, we estimated the pore diameter by probing with a range of anions and cations of different dimensions. Fig. 7 A shows data from the wild-type receptor. The filled symbols represent cation substitutions and the open symbols represent anion substitutions. For all the graphs in Fig. 7, the dotted and dashed lines are the predicted "ideal" reversal potentials from the calculated relative permeabilities presented earlier, assuming the substituted anion or cation was totally impermeant. From Fig. 7 A, we see that the shift in reversal potential reaches its maximum with an anion diameter between 4 and 6 Å. This agrees with the previous estimation of 6 Å determined by fitting anion permeabilities as a function of size (Wotring et al., 1999). Except for an apparent anomalous effect with cesium (3.4 Å), cation substitution did not shift the observed reversal potential in the wild-type receptor. Fig. 7 (B–F) shows substitution experiments for glutamate mutations from positions P290 through P294. Remember that positions 290, 292, and 294 showed the greatest permeation of cations, while 291 and 293 were less cation permeant. From these approximations it seems that, in all cases, reversal potential shifts approach their maximum with an ionic diameter between 4 and 6 Å. These findings suggest that the glutamate substitutions do not alter the diameter of the pore to any significant degree.

DISCUSSION

The Cys-loop superfamily offers a unique opportunity for investigating selectivity structure and mechanisms since there is substantial sequence homology, yet members of this receptor family include both cationic- and anionic-selective pores. To date, several charged residues at the cytoplasmic, intermediate, and extracellular locations of TM2 have been implicated in ion selectivity (Konno et al., 1991; Galzi et al., 1992; Keramidas et al., 2000; Gunthorpe and Lummis, 2001; Jensen et al., 2002; Thompson and Lummis, 2003; Menard et al., 2005). In a previous report, we expanded the mutagenesis studies to include the ρ1 homomeric GABA receptor (Wotring et al., 2003). Here, we extend the potential determinants of ionic selectivity to include a seven–amino acid stretch near the intracellular end of the pore.

Glutamate Scan Suggests a β-Strand Structure

Within the seven amino acid domain, an intriguing pattern emerged, and is shown in Fig. 5. At roughly every other site, glutamate substitution resulted in cation-preferring receptors. These cation mutants alternated with

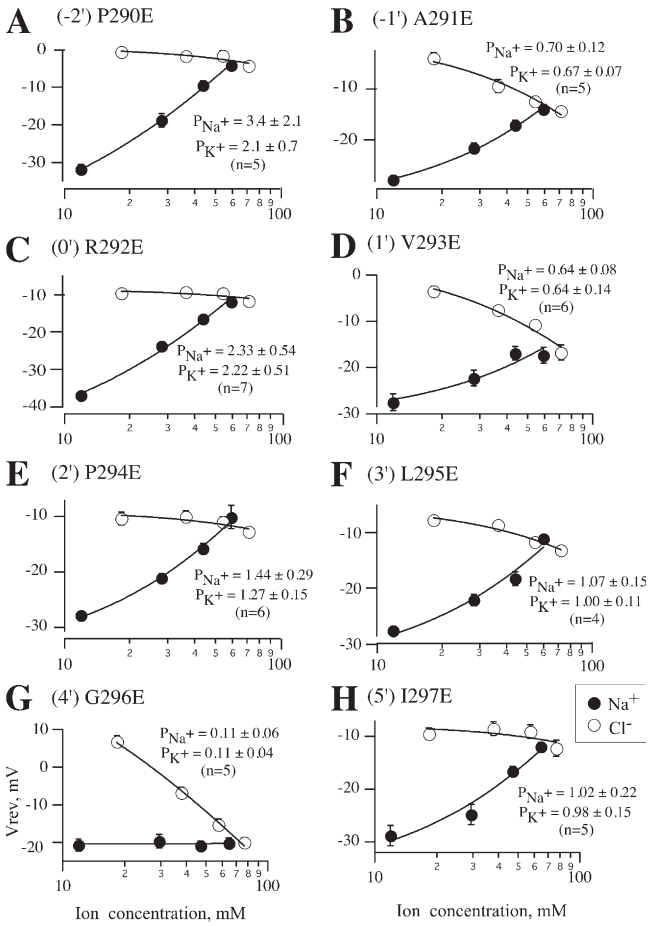

Figure 4. Glutamate scanning reveals a pattern that alternates between cation and nonspecific permeability. (A–H) For each indicated glutamate mutant, reversal potentials were measured in solutions with different concentrations of sodium (solid) or chloride (open). Lines are GHK fits to the data. Reversal potentials were nearly unaffected by chloride concentration in mutants that are cation preferring (A, C, and E), while for nonselective mutants the reversal potentials were shifted by changes in sodium or chloride concentration (B, D, G, and H). Systematic substitution of glutamate for each amino acid from −2' to 5′ exhibited a nearly alternating pattern of cation-preferring receptors and nonselective receptors.

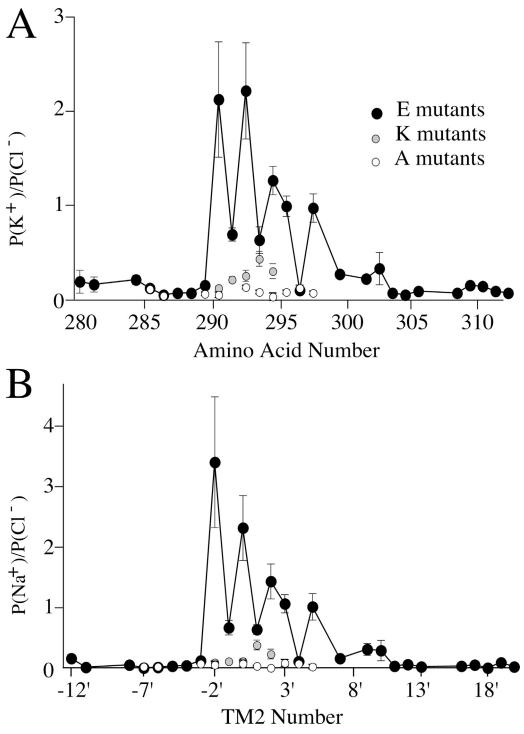

Figure 5. Alternate glutamate mutants at the intracellular end of TM2 are cation preferring. (A) Relative potassium permeability plotted against amino acid number shows the alternating pattern of cationic glutamate mutants (solid circles). Substitutions by positive lysine residues (gray circles) resulted in only small increases in potassium permeability. Substitution by neutral alanines (open circles) had no significant effect on ionic permeabilities. (B) Same as A, showing relative sodium permeability of mutant receptors.

mutants exhibiting a charge nonspecific or unchanged selectivity. This alternating pattern is consistent with a β-strand structure. Mutagenesis-induced cation permeability peaked at the −2' position, tapering off as the charged residue was moved up into the channel lumen toward the extracellular space. Our functional assay demonstrates that each residue from −2' to 5′, excluding 4', is capable of altering ionic permeability when mutated to glutamate.

It has long been assumed that most ion channel transmembrane domains are helical, but there is some evidence to the contrary. Molecular modeling using several structural prediction algorithms and incorporating data from many Cys-loop receptor subunits has suggested that the intracellular end of TM2 may form a β-strand (Le Novere et al., 1999). More specifically, based on an alignment between the α7 examined in that study with ρ1, their β-strand would extend from 0' to 6' with the structure of the upstream sequence not defined. In another recent modeling study, it was proposed that the TM2 helix of GABA α1 begins at the 3′–4' residues, leaving the more intracellular portion nonhelical (Bertaccini and Trudell, 2002). However, the computer algorithms that form the basis of most structural modeling or prediction programs make specific, and ill-defined, assumptions about the immediate environment (protein, aqueous, lipid). Our conclusion that this region is a β-strand will therefore remain a working hypothesis.

Comparison with Other Cys-Loop Receptors

One might expect that charge substitution of amino acids that line the lumen of the ion pathway would have a greater influence on ion permeation and selectivity compared with those residues that face away from the pore. This assumption depends upon the local architecture (e.g., diameter) and electrostatics. In addition to these assumptions, alignment between the TM1–TM2 linker and TM2 regions can be problematic, especially between cationic and anionic members of this receptor family,

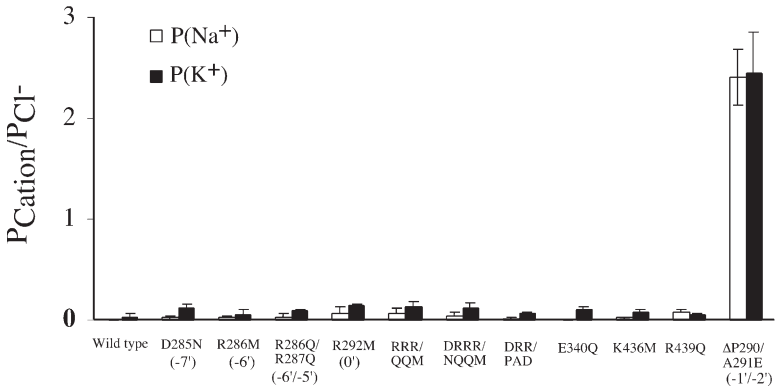

Figure 6. Endogenous charged residues in the wild-type receptor have little effect on ionic permeability. Charged amino acids at the intracellular membrane interface were neutralized to examine the role of native charges on ionic permeability. Although small elevations in relative cation permeability were evident, none of the constructs increased relative cation permeability to more than 0.15, in stark contrast to the previously described deletion of P290 and mutation of A291 to E (ΔP290/A291E), shown for comparison (Wotring et al., 2003). RRR/QQM is R286Q/R287Q/R292M, DRRR/NQQM is D285N/R286Q/R287Q/R292M, and DRR/PAD is D285P/R286A/R287D. For the latter case, the mutations were to the corresponding sequence in nAChR rather than a simple neutralization.

since the −2' proline in the GABA receptor is deemed missing in the cationic Cys-loop receptors. And lastly, the ρ1 GABA receptor differs from other members of this family in that it also contains a proline at the 2' position rather than the more typical serine or threonine.

It is tempting to compare our findings with studies using the substituted cysteine accessibility method (SCAM) that can identify putative pore-lining amino acids (Karlin and Akabas, 1998). The ρ1 GABA receptor residues that showed the greatest propensity to conduct cations when mutated to glutamate were the proline, arginine, and proline at the −2, 0', and 2' positions, respectively. As discussed above, the nACh and 5-HT_3 receptors do not have the proline at the −2 position, but rather have a glycine present. SCAM studies in which reagents were added extracellularly demonstrated that only the 2' position (among the −2, 0, and 2' positions) was accessible (Akabas et al., 1992, 1994; Reeves et al., 2001). However, SCAM studies of the nACh receptor in which reagents were added intracellularly, revealed modification at the −2' and 0' positions in the presence of agonist (Wilson and Karlin, 1998). In the present study, the introduction of a glutamate at the 2' position did increase the cation permeability, although to a lesser extent than at positions deeper into TM2 (−2'). Early mutagenesis experiments in the nACh receptor suggested the 2' position may be the narrowest portion of the pore (Konno et al., 1991; Villarroel et al., 1991; Cohen et al., 1992a,b), so one might have expected a greater electrostatic interaction with the permeant ion and hence a greater effect on selectivity. Previous SCAM studies in the ρ1 receptor, however, revealed modification of the −2' position, demonstrating differences in accessibility profiles even between GABA receptors (Filippova et al., 2004). The −2' position has also been implicated as a contributor of pore diameter and ion selectivity in the glycine receptor (Lee et al., 2003).

Glutamate substitutions at the −1', 0', 3′, and 5′ positions produced more modest changes in selectivity, resulting in essentially comparable degrees of cation and anion permeation. None of these positions were accessible in the α1 subunit of α1β1γ2 GABA receptors (Xu and Akabas, 1996), but the 1' position was accessible in the ρ1 receptor (Filippova et al., 2004). If this region were a β-strand as suggested above, then perhaps it follows that charges in side chains that face away from the pore have less of an impact on selectivity than those that face the lumen. In this study, we are examining the ability of the pore to select between ions that differ in charge but exist over a limited size range, and therefore one must be cautious when extrapolating these data to pore architecture. SCAM analysis, on the other hand, is comparing the ability of modifying reagents to reach and react with introduced cysteines. In this case, the absence of modification might reflect inaccessibility of the reagent (size selection) rather than position of the side chain with respect to the pore. That is, the reagents may not be able to access the narrowest regions of the pore.

Our data also indicated minimal, if any, changes in pore diameter regardless of the charge selectivity. For example, the −2E' and 0E' mutants (the most cation-permeant receptors in the present study) demonstrated a wild-type pore diameter when probed with cations of different sizes (Fig. 5, B and C). This was surprising since cationic-selective members of the Cys-loop family (Dwyer et al., 1980; Yang, 1990; Cohen et al., 1992b) appear to have larger pore diameters than the anionic-selective members (Bormann et al., 1987; Fatima-Shad and Barry, 1993; Wotring et al., 1999; Keramidas et al., 2002), although the degree of cation selectivity in our mutants is less than that of the "true" cationic receptors. In addition, studies in the glycine receptor indicated an apparent increase in the pore diameter concomitant with the increased cation selectivity imparted by mutagenesis (Keramidas et al., 2002). The extent to which these differences between glycine and ρ1 GABA receptors reflect differences in pore structure, or rather the methodology for estimating the pore diameter, is presently unclear.

In any mutagenesis study, one must proceed with caution when interpreting the impacts of a structural change. In an effort to address this possibility, we did follow up our glutamate substitutions with alanine mutations to

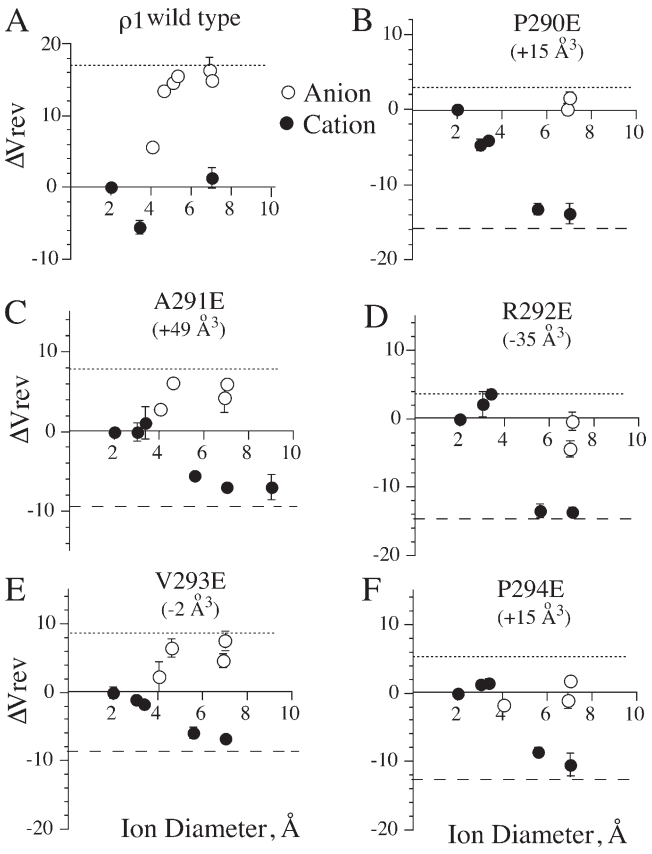

Figure 7. Glutamate substitutions do not alter the apparent pore size. (A–F) Reversal potentials were measured after substitution with anions (open symbols) and cations (closed symbols) of different diameters. The dashed and dotted lines indicate the calculated reversal potential shift for an impermeant anion or cation, respectively, and were based on the determined relative permeabilities for that particular mutant. For the wild-type receptor, the reversal potential shift approaches its maximum value for anions between 4 and 6 Å. Using this approximation, the data indicate that for all cases, the pore size was between 4 and 6 Å. The cations and their diameters (in Å) were as follows: cations, sodium, 1.9; rubidium, 3.0; cesium, 3.4; imadazole, 4.8; choline, 5.6; triethanolamine, 7.0; *N*-methyl-D-glucamine, 9.0; anions, bicarbonate, 4.1; acetate, 4.5; propionate, 5.1; gluconate, 6.9; isethionate, 7.0. Under the particular mutation, we provide the difference in side chain volume imparted by the substitution.

assess a structural perturbation, and lysine mutations to assess the introduction of a charge, but to a sign opposite that of glutamate (Fig. 5). While the alanine substitutions in our region of interest had either minimal, or no, impact on selectivity, the lysine substitutions showed a significant increase in cation permeability. This increase in cation permeability was still much less than that of the glutamate substitutions at these positions. For example, in all cases, the lysine substitutions were still more permeable to anions than cations. Further mutagenesis would have to be performed in an attempt to dissect out the contributing factor(s) (e.g., charge versus size) and the extent to which the effects on selectivity for the glutamate mutations represent electrostatic interactions with the permeating ions. Finally, at physiological pH, glutamate would be deprotonated and hence negatively charged. However, without knowing the "microclimate" around the side chain with such complicating factors as surface charge and hydrophobicity, it is unknown how many of the five glutamates would be deprotonated.

Is Part of the Permeation Pathway in an Intracellular Portion of the Protein?

It is generally assumed that the amino acids that form the pore, and thus the ionic permeation pathway, lie within the cell membrane. Hydropathy plots and sequence alignments indicate that at least part of the –2' to 5′ span lies in the intracellular loop between TM1 and TM2, and therefore would not be expected to be part of the "classic" TM2 pore. Structural models of a nicotinic acetylcholine receptor show that a portion of the ion pathway is formed by an intracellular part of the channel protein, referred to as a fenestrated hanging gondola (Miyazawa et al., 1999) and later termed the intracellular vestibule (Unwin, 2005). Lateral windows in this structure provide several openings that permeating ions can pass through, and there are many negatively charged residues near these openings in the cation-selective nACh channel. In a previous study, we used cysteine mutants and charged sulfhydryl reagents to show that portions of the TM1–TM2 linker, and even TM1 itself, lie within the permeation pathway (Filippova et al., 2004), and this was confirmed in the nACh structural model. The results we describe here are in agreement with Cys-loop structural models that incorporate an intracellular extension of the pore formed by cytoplasmic portions of the protein. That our charge scanning upstream from −2' did not alter ion selectivity suggests that if this region does form an extension of the pore, it is likely not a narrow segment.

The wild-type ρ1 receptor exhibited a permeability ratio of 33 ($P_{Cl-/K+}$), while the mutation that imparted the greatest permeability for cations (P2'E) exhibited a permeability ratio of only 3.4 ($P_{Na+/Cl-}$). Although cation preferring, this is less stringent of a selectivity then wild-type cationic members of this Cys-looop family. For example, the 5-HT_{3A} receptor displays a $P_{Na+/Cl-}$ value of 53 (Thompson and Lummis, 2003) and the α7 nACh receptor has a reported $P_{K+/Cl-}$ value of ≈20 (Bertrand et al., 1993). In all cases where mutations have been produced in this region in an effort to invert the selectivity, the degree of inverted selectivity has fell short of wild-type anionic and cationic members of this family and comparable to what we observed here (Galzi et al., 1992; Keramidas et al., 2000; Gunthorpe and Lummis, 2001; Keramidas et al., 2002; Thompson and Lummis, 2003; Wotring et al., 2003). A likely interpretation of this observation is that other regions contribute to ion

selectivity, and specific regions have been proposed (Galzi et al., 1991; Cohen et al., 1992b; Unwin, 2005). Even if the region investigated here was the sole determinant of charge selectivity for permeating ions, there are sequence (and hence structural) differences in neighboring regions making it unlikely that site-directed mutagenesis would recapitulate the proper pore structure necessary for the exquisite selectivity of wild-type receptors.

Comparing Mechanisms that Control Cation and Anion Selectivity

The experimental observation that substitutions at homologous positions can influence the selectivity of anionic or cationic members of this Cys-loop superfamily argues that the position of the region(s) that determines ion selectivity is well conserved (Galzi et al., 1992; Corringer et al., 1999; Keramidas et al., 2000; Keramidas et al., 2002; Thompson and Lummis, 2003; Wotring et al., 2003). The experiments described here show that one can confer cation permeability to an anion-selective channel by introducing negatively charged residues at key locations. It might then follow that positively charged residues in the same region would result in anion permeability, but our charge neutralization experiments refute this hypothesis, at least for the −2' to 5′ domain. If the ancestral Cys-loop receptor was indeed an anion channel (Ortells and Lunt, 1995), relatively small mutations like the glutamate substitutions described in this report could have resulted in cation-selective channels.

Although it is difficult to elucidate the mechanism of ion selectivity in the absence of definitive structural information, the experiments described above provide some leads. The effects of glutamate substitution on ionic selectivity support an electrostatic mechanism rather than a molecular sieve model. In addition, the alternating pattern of mutagenesis-induced cation permeability suggests a β-strand structure toward the intracellular end of the pore. Finally, the observation that the mutations in this domain did not alter the estimated pore size suggests that the region of the permeation pathway that defines the minimal pore diameter is either located elsewhere or is highly constrained by neighboring protein segments (i.e., held rigid).

This work was supported by National Institutes of Health grant NS35291 (D.S. Weiss).

Olaf S. Andersen served as editor.

Submitted: 13 November 2006
Accepted: 23 November 2007

REFERENCES

Akabas, M.H., D.A. Stauffer, M. Xu, and A. Karlin. 1992. Acetylcholine receptor channel structure probed in cysteine-substitution mutants. *Science.* 258:307–310.

Akabas, M.H., C. Kaufmann, P. Archdeacon, and A. Karlin. 1994. Identification of acetylcholine receptor channel-lining residues in the entire M2 segment of the rho subunit. *Neuron.* 13:919–927.

Amin, J., and D.S. Weiss. 1994. Homomeric rho1 GABA channels: activation properties and domains. *Receptors Channels.* 2:227–236.

Bertaccini, E., and J.R. Trudell. 2002. Predicting the transmembrane secondary structure of ligand-gated ion channels. *Protein Eng.* 15:443–454.

Bertrand, D., J.L. Galzi, A. Devillers-Thiery, S. Bertrand, and J.P. Changeux. 1993. Mutations at two distinct sites within the channel domain M2 alter calcium permeability of neuronal α7 nicotinic receptor. *Proc. Natl. Acad. Sci. USA.* 90:6971–6975.

Bormann, J., O.P. Hamill, and B. Sakmann. 1987. Mechanism of ion permeation through channels gated by glycine and γ-aminobutyric acid in mouse cultured spinal neurones. *J. Physiol.* 385:243–286.

Cohen, B.N., C. Labarca, L. Czyzyk, N. Davidson, and H.A. Lester. 1992a. $Tris^+/Na^+$ permeability ratios of nicotinic acetylcholine receptors are reduced by mutations near the intracellular end of the M2 region. *J. Gen. Physiol.* 99:545–572.

Cohen, B.N., C. Labarca, N. Davidson, and H.A. Lester. 1992b. Mutations in M2 alter the selectivity of the mouse nicotinic acetylcholine receptor for organic and alkali metal cations. *J. Gen. Physiol.* 100:373–400.

Corringer, P.-J., S. Bertrand, J.L. Galzi, A. Devillers-Thiery, J.P. Changeux, and D. Bertrand. 1999. Mutational analysis of the charge selectivity of the α7 nicotinic acetylcholine receptor. *Neuron.* 22:831–843.

Dwyer, T.M., D.J. Adams, and B. Hille. 1980. The permeability of the endplate channel to organic cations in frog muscle. *J. Gen. Physiol.* 75:469–492.

Fatima-Shad, K., and P. Barry. 1993. Anion permeation in GABA- and glycine-gated channels of mammalian cultured hippocampal neurons. *Proc. R. Soc. Lond. B. Biol. Sci.* 253:69–75.

Filippova, N., V.E. Wotring, and D.S. Weiss. 2004. Evidence that the TM1-TM2 loop contributes to the ρ1 GABA receptor pore. *J. Biol. Chem.* 279:20906–20914.

Galzi, J., D. Bertrand, A. Devillers-thiery, F. Revah, S. Bertrand, and J. Changeux. 1991. Functional significance of aromatic amino acids from three peptide loops of the α7 neuronal nicotinic receptor site investigated by site-directed mutagenesis. *FEBS Lett.* 294:198–202.

Galzi, J.L., A. Devillers-Thiery, N. Hussy, S. Bertrand, J.P. Changeux, and D. Bertrand. 1992. Mutations in the ion channel domain of a neuronal nicotinic receptor convert ion selectivity from cationic to anionic. *Nature.* 359:500–505.

Giraudat, J., M. Dennis, T. Heidmann, J.Y. Chang, and J.P. Changeux. 1986. Structure of the high-affinity binding site for noncompetitive blockers of the acetylcholine receptor: serine-262 of the δ subunit is labeled by [3H]chlorpromazine. *Proc. Natl. Acad. Sci. USA.* 83:2719–2723.

Goldman, D. 1943. Potential, impedance, and rectification in membranes. *J. Gen. Physiol.* 27:37–60.

Gunthorpe, M.J., and S.C. Lummis. 2001. Conversion of the ion selectivity of the 5-HT(3a) receptor from cationic to anionic reveals a conserved feature of the ligand-gated ion channel superfamily. *J. Biol. Chem.* 276:10977–10983.

Hodgkin, A.L., and B. Katz. 1949. The effect of temperature on the electrical activity of the giant axon of the squid. *J. Physiol.* 109:240–249.

Hucho, F., W. Oberthur, and F. Lottspeich. 1986. The ion channel of the nicotinic acetylcholine receptor is formed by the homologous helices M II of the receptor subunits. *FEBS Lett.* 205:137–142.

Jensen, M.L., D.B. Timmermann, T.H. Johansen, A. Schousboe, T. Varming, and P.K. Ahring. 2002. The β subunit determines the ion selectivity of the GABAA receptor. *J. Biol. Chem.* 277:41438–41447.

Kammann, M., J. Laufs, J. Schell, and B. Gronenborn. 1989. Rapid insertional mutagenesis of DNA by polymerase chain reaction (PCR). *Nucleic Acids Res.* 12:4445–4452.

Karlin, A., and M.H. Akabas. 1998. Substituted cysteine accessibility method. *Methods Enzymol.* 293:123–145.

Keramidas, A., A.J. Moorhouse, C.R. French, P.R. Schofield, and P.H. Barry. 2000. M2 pore mutations convert the glycine receptor channel from being anion- to cation-selective. *Biophys. J.* 79:247–259.

Keramidas, A., A.J. Moorhouse, K.D. Pierce, P.R. Schofield, and P.H. Barry. 2002. Cation-selective mutations in the M2 domain of the inhibitory glycine receptor channel reveal determinants of ion-charge selectivity. *J. Gen. Physiol.* 119:393–410.

Konno, T., C. Busch, E. Von Kitzing, K. Imoto, F. Wang, J. Nakai, M. Mishina, S. Numa, and B. Sakmann. 1991. Rings of anionic amino acids as structural determinants of ion selectivity in the acetylcholine receptor channel. *Proc. Biol. Sci.* 244:69–79.

Le Novere, N., P.J. Corringer, and J.P. Changeux. 1999. Improved secondary structure predictions for a nicotinic receptor subunit: incorporation of solvent accessibility and experimental data into a two-dimensional representation. *Biophys. J.* 76:2329–2345.

Lee, D.J., A. Keramidas, A.J. Moorhouse, P.R. Schofield, and P.H. Barry. 2003. The contribution of proline 250 (P-2') to pore diameter and ion selectivity in the human glycine receptor channel. *Neurosci. Lett.* 351:196–200.

Leonard, R.J., C.G. Labarca, P. Charnet, N. Davidson, and H.A. Lester. 1988. Evidence that the M2 membrane-spanning region lines the ion channel pore of the nicotinic receptor. *Science.* 242:1578–1581.

Liman, E.R., P. Hess, F. Weaver, and G. Koren. 1991. Voltage-sensing residues in the S4 region of a mammalian K+ channel. *Nature.* 353:752–756.

Marcus, Y. 1997. Ion Properties. Marcel Dekker, New York. 43–62.

Menard, C., H.R. Horvitz, and S. Cannon. 2005. Chimeric mutations in the M2 segment of the 5-hydroxytryptamine-gated chloride channel MOD-1 define a minimal determinant of anion/cation permeability. *J. Biol. Chem.* 280:27502–27507.

Miyazawa, A., Y. Fujiyoshi, M. Stowell, and N. Unwin. 1999. Nicotinic acetylcholine receptor at 4.6 Å resolution: transverse tunnels in the channel wall. *J. Mol. Biol.* 288:765–786.

Ortells, M.O., and G.G. Lunt. 1995. Evolutionary history of the ligand-gated ion-channel superfamily of receptors. *Trends Neurosci.* 18:121–127.

Reeves, D.C., E.N. Goren, M.H. Akabas, and S.C. Lummis. 2001. Structural and electrostatic properties of the 5-HT3 receptor pore revealed by substituted cysteine accessibility mutagenesis. *J. Biol. Chem.* 276:42035–42042.

Thompson, A.J., and S.C. Lummis. 2003. A single ring of charged amino acids at one end of the pore can control ion selectivity in the 5-HT3 receptor. *Br. J. Pharmacol.* 140:359–365.

Unwin, N. 2005. Refined structure of the nicotinic acetylcholine receptor at 4 Å resolution. *J. Mol. Biol.* 346:967–989.

Villarroel, A., S. Herlitze, M. Koenen, and B. Sakmann. 1991. Location of a threonine residue in the α-subunit M2 transmembrane segment that determines the ion flow through the ion flow through the acetylcholine receptor channel. *Proc. Biol. Sci.* 243:69–74.

Wilson, G.G., and A. Karlin. 1998. The location of the gate in the acetylcholine receptor channel. *Neuron.* 20:1269–1281.

Wotring, V.E., Y. Chang, and D.S. Weiss. 1999. Permeability and selectivity of human homomeric ρ1 $GABA_C$ receptors. *J. Physiol.* 521:327–336.

Wotring, V.E., T.S. Miller, and D.S. Weiss. 2003. Mutations at the GABA receptor selectivity filter: a possible role for effective charges. *J. Physiol.* 548:527–540.

Xu, M., and M.H. Akabas. 1996. Identification of channel-lining residues in the M2 membrane-spanning segment of the $GABA_A$ receptor ρ1 subunit. *J. Gen. Physiol.* 107:195–205.

Yang, J. 1990. Ion permeation through 5-hydroxytryptamine–gated channels in neuroblastoma N18 cells. *J. Gen. Physiol.* 96:1177–1198.